

To the theory of rare gas alloys: heat capacity

Cite as: *Low Temp. Phys.* **33**, 564 (2007); <https://doi.org/10.1063/1.2755174>
 Published Online: 24 July 2007

M. I. Bagatskii, S. B. Feodosyev, I. A. Gospodarev, O. V. Kotlyar, E. V. Manzhelii, A. V. Nedzvetskiy, and E. S. Syrkin



[View Online](#)



[Export Citation](#)

ARTICLES YOU MAY BE INTERESTED IN

[Evolution of discrete local levels into an impurity band in solidified inert gas solution](#)
Low Temperature Physics **33**, 559 (2007); <https://doi.org/10.1063/1.2746251>

[Phonon heat capacity of graphene nanofilms and nanotubes](#)
Low Temperature Physics **43**, 264 (2017); <https://doi.org/10.1063/1.4978291>

LOW TEMPERATURE TECHNIQUES
OPTICAL CAVITY PHYSICS
 MITIGATING THERMAL
 & VIBRATIONAL NOISE

DOWNLOAD THE WHITE PAPER

downloads.montanainstruments.com/optical_cavities

MONTANA INSTRUMENTS
 COLD SCIENCE MADE SIMPLE



To the theory of rare gas alloys: heat capacity

M. I. Bagatskii, S. B. Feodosyev,^{a)} I. A. Gospodarev, O. V. Kotlyar, E. V. Manzhelii, A. V. Nedzvetskiy, and E. S. Syrkin

B. Verkin Institute for Low Temperature Physics and Engineering of the National Academy of Sciences of Ukraine 47 Lenin Ave., Kharkov 61103, Ukraine
(Submitted October 20, 2006)

Fiz. Nizk. Temp. **33**, 741–746 (June–July 2007)

The low-temperature heat capacity of cryocrystals containing impurity clusters is investigated theoretically and experimentally. Such defects might essentially enrich the low-frequency part of the phonon spectrum by introducing both localized and delocalized vibrations. The effect of both types of vibrations on the temperature dependence of the heat capacity is analyzed. The heat capacity of the disordered solid solution Kr–Ar (Ar concentration $\sim 25\%$) is studied as an example of the effect of the light, weakly coupled impurities on the low-temperature thermodynamic characteristics of a system. The mass defect of such an impurity induces “phonon pumping” from the low-frequency part of the spectrum into the high-frequency part and decreases the low-temperature heat capacity, while the weakened interaction between the impurity and the host atoms, combined with even weaker interaction between the impurities, leads to the formation of a low-temperature maximum on the heat capacity temperature dependence. The analysis performed shows that at rather high Ar concentrations, the nonmonotonic temperature dependence of the relative change in the heat capacity of $\text{Kr}_{1-p}\text{Ar}_p$ solid solutions is a result of the excitation of delocalized high-dispersion low-frequency phonons. © 2007 American Institute of Physics.

[DOI: [10.1063/1.2755174](https://doi.org/10.1063/1.2755174)]

INTRODUCTION

For many years the influence of defects on the physical properties of cryocrystals has been one of the most important problems of the low-temperature physics of solids and has stimulated intense theoretical and experimental research (e.g., see monograph¹ and references therein). The results obtained on such objects are explainable with high accuracy within quite simple crystal lattice models and can be generalized for a very wide class of crystalline structures.

At present there is a practically complete theory interpreting the variations of the crystal properties caused by the so-called isolated defects, whose influence upon one another is negligible. It is certainly interesting to investigate crystals with defects that can be classified as complex ones, for example, impurities located near a sample boundary or a vacancy. When the concentration of impurity atoms in the lattice grows, complex defects can appear in addition to the isolated ones. Complex defects are formed by closely spaced impurities. In some cases they may be considered as isolated defects^{2–5} and can be described using regular perturbation theory.

Special interest is focused on systems consisting of a cryocrystalline matrix containing randomly dissolved impurity atoms. At a growing concentration the spectral characteristics of such solutions exhibit properties that are typical of amorphous compounds, glasses, biopolymers, and so on. One of the features characterizing such systems is the anomalous frequency distribution of phonons in the long-wavelength (low-frequency) region. This is evident in Raman and neutron scattering experiments^{6–8} and in the behavior of the low-temperature heat capacity and thermal conductivity.^{9–11}

This anomaly of the frequency distribution of phonons can be described as a maximum of the magnitude $I \equiv g(\omega)/\omega^2$, where $g(\omega)$ is the phonon density of states and ω is the frequency. The maximum was called a “boson peak.” It is typical for glasses, amorphous media, and other disordered systems in which the influence of defects goes beyond local disturbances. The change in the vibrational and other physical properties of such systems cannot be interpreted as regular degenerate perturbation.

In this study we investigate theoretically how the low-temperature heat capacity of $\text{Kr}_{1-p}\text{Ar}_p$ solid solutions changes at growing concentration p of Ar atoms. Argon and krypton are highly soluble in each other and the parameter p can take any value varying from zero to unity.¹² The calculated results are compared with the currently available experimental data. It is shown that the change in the low-temperature heat capacity at argon concentrations $p \geq 20\%$ and lower ($\sim 5\text{--}10\%$) has qualitative features induced by delocalized excitations, analogous to boson peaks, that appear in addition to the local (including complex) defects.

CHANGES IN HEAT CAPACITY OF KRYPTON CAUSED BY ARGON IMPURITY

We develop a model crystal lattice of the $\text{Kr}_{1-p}\text{Ar}_p$ system on the basis of the fcc structure with the lattice parameter of pure krypton ($a \approx 5.59 \text{ \AA}$).¹ In our description the interatomic interaction in solidified inert gases is reduced to the interaction between the nearest neighbors. In the general case this interaction is characterized by three force constants α , β , and γ :

$$\Phi_{ik}\left(\frac{a}{2}; \frac{a}{2}; 0\right) = \begin{pmatrix} \alpha & \gamma & 0 \\ \gamma & \alpha & 0 \\ 0 & 0 & \beta \end{pmatrix}. \quad (1)$$

The other force constant matrices can be found from Eq. (1) by O_h -group symmetry operations, and the matrix of self-action is

$$\Phi_{ik}(0; 0; 0) = (8\alpha + 4\beta)\delta_{ik}. \quad (2)$$

Since a crystal of cubic symmetry has three independent elastic moduli, C_{11} , C_{12} , and C_{66} , we can use their values and estimate unambiguously the force constants α , β , and γ . For krypton¹³ we obtain $\alpha_{\text{Kr-Kr}} = 7260.3$ dyn/cm, $\beta_{\text{Kr-Kr}} = 310.75$ dyn/cm, $\gamma_{\text{Kr-Kr}} = 7797.0$ dyn/cm. The force constants characterizing the Kr–Ar and Ar–Ar interactions can be calculated with help of the Lennard-Jones potentials (with the parameters ε and σ for Kr and Ar, see, e.g., Ref. 1):

$$\alpha_{\text{Kr-Ar}} = 7804.0, \quad \beta_{\text{Kr-Ar}} = 127.00, \quad \gamma_{\text{Kr-Ar}} = 7310.0;$$

$$\alpha_{\text{Ar-Ar}} = 1551.83, \quad \beta_{\text{Ar-Ar}} = 220.677,$$

$$\gamma_{\text{Ar-Ar}} = 1331.15.$$

We assume that the Ar–Ar interaction is the same for the nearest Ar pairs and the larger clusters of defects (triangles, tetrahedrons, etc.) that can form as the Ar concentration increases.

The calculations performed in this study are based on the \mathcal{J} -matrix technique (see, e.g., Refs. 14–16). The method does not use explicitly the translational symmetry of the crystal lattice and permits a straightforward calculation of the spectral densities corresponding to the displacements of different atoms of the system along different crystallographic directions i :

$$\rho_i(\omega, \mathbf{r}) = \frac{1}{\pi} \text{Im } \mathcal{G}_i(\omega, \mathbf{r}). \quad (3)$$

Here \mathbf{r} is the radius vector characterizing the position of the particular atom, ω is the frequency, and the Green function $\mathcal{G}_i(\omega, \mathbf{r})$ is expressed in terms of the matrix element of the resolvent operator as follows:

$$\mathcal{G}_i(\omega, \mathbf{r}) = 2\omega \cdot \left\langle \begin{matrix} \mathbf{r} \\ u_i \end{matrix} \left| (\omega^2 \hat{\mathcal{I}} - \hat{\mathcal{L}})^{-1} \right| \begin{matrix} \mathbf{r} \\ u_i \end{matrix} \right\rangle \quad (4)$$

where the symbol $\left\langle \begin{matrix} \mathbf{r} \\ u_i \end{matrix} \right|$ has the meaning of the displacement of the atom with the radius vector \mathbf{r} along the crystallographic direction i (a certain vector in the space of atom displacements in the system H); $\hat{\mathcal{I}}$ is the unit operator, and $\hat{\mathcal{L}}$ is the operator describing the atomic oscillations in the system; its eigenvalues are the squared eigenfrequencies. The matrix of this operator can be expressed in terms of the force constant matrix and the masses of the interacting atoms $m(\mathbf{r})$ and $m(\mathbf{r}')$.

The spectral density of the system is

$$\langle \rho(\omega, p) \rangle = \lim_{N \rightarrow \infty} \frac{2\omega}{\pi N} \text{Tr } \text{Im}(\omega^2 \hat{\mathcal{I}} - \hat{\mathcal{L}})^{-1}. \quad (5)$$

According to Refs. 17–20, it is a self-averaging quantity and can be estimated through averaging the functions over all positions \mathbf{r} and displacement directions i .

The random distribution of the Ar impurity atoms was performed using a random number generator of pseudorandom numbers distributed uniformly in the interval (0, 1). The random number generator operates on the multiplying congruent principle.²¹ We calculated the spectral densities $\langle \rho(\omega, p) \rangle$ for different concentrations of impurity atoms. At each concentration, the averaging was done over several thousand random configurations of the impurity distribution. For each configuration the density of states was determined through averaging over several tens of spectral densities corresponding to the displacements along different crystallographic directions of several tens of sequentially arranged atoms.

The vibrational heat capacity C_v (heat capacity at constant volume) is expressed in terms of the phonon density as (see, e.g., Ref. 22) of solid solutions is expressed in terms of $\nu(\omega)$ as

$$C_v(T, p) = 3R \int_{\mathcal{D}} \left(\frac{\hbar\omega}{kT} \right)^2 \sinh^{-2} \left(\frac{\hbar\omega}{kT} \right) \nu(\omega) d\omega, \quad (6)$$

where the integral is calculated in the whole region of the atomic oscillation frequencies \mathcal{D} both over the quasi-continuous spectrum band and over the discrete levels (if there are any).

We obtain $\nu(\omega) = \langle \rho_i(\omega, p) \rangle$ for solid solutions and $\nu(\omega) = \rho_i(\omega, \forall \mathbf{r})$ for a perfect single-atom crystal lattice of cubic symmetry. The function $\rho_i(\omega, \forall \mathbf{r})$ is the spectral density caused by the displacement of an arbitrary atom in any of the crystallographic directions.

It is known that at low concentrations the interaction between the impurity atoms is negligible. It is also assumed that the impurity-induced change in the additive thermodynamic characteristics is linear in the impurity concentration p . Thus, at $p \ll 1$

$$\frac{\Delta C_v(T, p)}{C_v^{(\text{Kr})}(T)} \approx p \frac{\Delta C_v^l(T)}{C_v^{(\text{Kr})}(T)},$$

where $\Delta C_v^l(T)$ is the change in the heat capacity per local defect. The disturbance of the lattice vibrations generated by a local defect is, as a rule, localized around that defect.

The $C_v^l(T)$ value can be calculated using, for example, a shift function if the disturbance is regular and degenerate.^{23,24} According to the traditional interpretation of crystal lattice vibrations as a superposition of plane waves, only the disturbance generated by an isotopic impurity can be considered as degenerate (in three-dimensional vector models). The \mathcal{J} -matrix method treats the disturbance as degenerate if it is generated by an impurity with changed force constants in the case of a noncentral interaction between the atoms.²⁵ The presence of noncentral forces allows a distur-

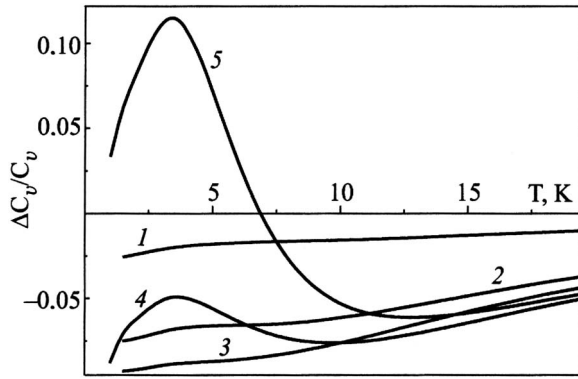


FIG. 1. Temperature dependences of the relative change in the heat capacity at a growing concentration of Ar impurity p [%]: 5 (1), 10 (2), 15 (3), 24.4 (4), 50 (5).

bance to be degenerate only in a subspace that can be transformed in one-dimensional representations of the symmetry group of the particular lattice.

At the same time, local disturbances do not affect the bandwidth of the quasi-continuous spectrum of the crystal. They can only form discrete local levels beyond the band. Therefore, the asymptotic behavior of the \mathcal{J} -matrix elements representing the operators $\hat{\mathcal{L}}$ that describe the lattice vibrations do not change under the influence of a local defect. It is natural to call such disturbances *asymptotically degenerate*.

Since the arbitrary matrix element $\mathcal{G}_{mn}(\omega^2)$ of the resolvent operator $\hat{\mathcal{G}}(\omega^2) \equiv (\omega^2 \hat{\mathcal{T}} - \hat{\mathcal{L}})^{-1}$ can be expressed straightforwardly through the element $\mathcal{G}_{00}(\omega^2) \equiv \mathcal{G}(\omega)$ (Green function), for $m < n$ we obtain⁵

$$\begin{aligned} \mathcal{G}_{mn}(\lambda) &\equiv (\mathbf{h}_m, \hat{\mathcal{G}}(\lambda) \mathbf{h}_n) = -\mathcal{P}_m(\lambda) \mathcal{Q}_n(\lambda) \\ &+ \mathcal{P}_m(\lambda) \mathcal{P}_n(\lambda) \mathcal{G}_{00}(\lambda), \end{aligned} \quad (7)$$

then the change in the heat capacity for such asymptotically degenerate local disturbance can be written in the form of the integral of Eq. (6) with the function $\nu(\omega)$ substituted by

$$\begin{aligned} \Delta \nu(\omega) &= 2\omega \sum_{n=0}^{r \rightarrow \infty} [\tilde{\mathcal{P}}_n^2(\omega^2) \tilde{\rho}(\omega^2) - \mathcal{P}_n^2(\omega^2) \rho(\omega^2)] \\ &+ \sum_l \delta(\omega - \omega_l). \end{aligned} \quad (8)$$

The second sum in Eq. (8) describes the contribution of local frequencies if they appear in the disturbed system; $\mathcal{P}_n(\omega^2)$ are the Jacobian matrix-generated polynomials (see, e.g., Ref. 14–16); the tilded variables refer to a disturbed system and can be calculated using the corresponding Jacobian matrix; the nontilded variables describe an ideal perfect lattice. The accuracy of computation by Eqs. (6) and (8) using a finite-rank \mathcal{J} matrix corresponds to the accuracy of calculation of the perfect-lattice heat capacity with the aid of the matrix of the same rank.

RESULTS AND DISCUSSION

By the methods above-mentioned we received the following results. Figure 1 illustrates the temperature dependences of the relative change

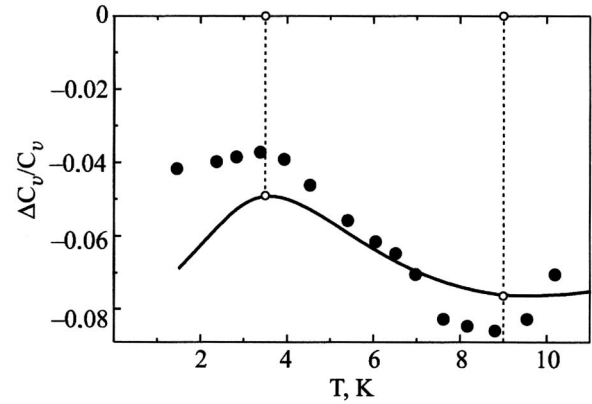


FIG. 2. Temperature dependences of the relative change in the heat capacity of a $\text{Kr}_{0.756}\text{Ar}_{0.244}$ solid solution: theoretical calculation (—), experiment (●).

$$\frac{\Delta C_v(T)}{C_v^{(\text{Kr})}(T)} \equiv \frac{\langle C_v(T, p) \rangle - C_v^{(\text{Kr})}(T)}{C_v^{(\text{Kr})}(T)}$$

in the heat capacity of $\text{Kr}_{1-p}\text{Ar}_p$ solid solutions with various Ar concentrations p in reference to the heat capacity of pure Kr.

The dependence is smooth at moderate p values (5 and 10%; curves 1 and 2, respectively). At $p=15\%$ (curve 3) the dependence exhibits some “flattening” in the interval $3.5 \text{ K} \leq T \leq 10 \text{ K}$. On a further increase in the Ar concentration: $p=24.4\%$ (curve 4) and 50% (curve 5), two extrema appear in $\Delta C_v(T, p)/C_v^{(\text{Kr})}(T)$ —a maximum at $T \approx 3.5 \text{ K}$ and a minimum at $T \approx 9 \text{ K}$ (24.4%) or $T \approx 12.5 \text{ K}$ (50%).

The measured temperature dependence of the relative change in the heat capacity at $p=24.4\%$ (●)²⁶ is shown in Fig. 2. There are two extrema in this case too: a maximum at $T \approx 3.5 \text{ K}$ and a minimum at $T \approx 9 \text{ K}$. The solid curve is a portion of the curve of Fig. 1, which illustrates a theoretical calculation of the same quantity at the same concentration. It is seen that the experimental and theoretical results are in good agreement—the temperatures of the extrema coincide with a high degree of accuracy and the deviations of $\Delta C_v(T, p)/C_v^{(\text{Kr})}(T)$ are actually within the accuracy of the experiment. True, the character of the dilation at these p values is more complicated than that allowed for in the model.

Let us analyze the possible reasons for the qualitative behavior of the relative change in the heat capacity with growing concentration.

Figure 3 illustrates the temperature dependence of the parameter $\Delta C_v^{1\text{Ar}}(T)/C_v^{(\text{Kr})}(T)$ describing the change in the heat capacity of Kr caused by an isolated atom of Ar impurity (curve 1) and of the parameter $\Delta C_v^{2\text{Ar}}(T)/C_v^{(\text{Kr})}(T)$ describing the change in the heat capacity caused by an isolated pair of adjacent Ar atoms (curve 2). The smooth rise of curve 1 with temperature and the very weak temperature dependence of curve 2 permit us to explain the heat capacity variation at low (down to 10%) concentrations of Ar impurity at the expense of a superposition of local disturbances localized near the defects¹⁾ that generate them. This explanation is totally unsuitable for the double extremum behavior of the parameter $\Delta C_v(T, p)/C_v^{(\text{Kr})}$ at higher concentrations.

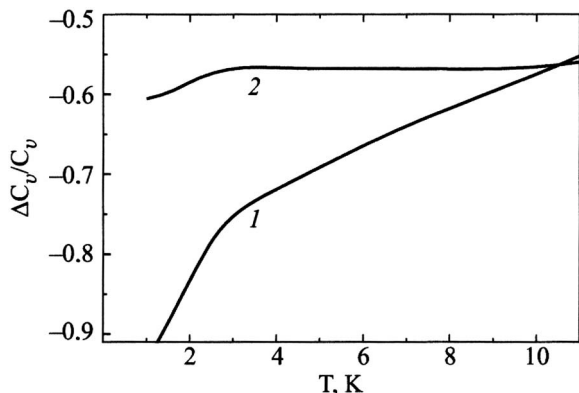


FIG. 3. Temperature dependences of the relative change in the heat capacity caused by an Ar substitutional impurity: curve 1—isolated Ar atom, curve 2—isolated pair of adjacent Ar atoms.

Since in the $Kr_{1-p}Ar_p$ solutions the linkage between the Ar atoms is much weaker than the Kr–Kr or Kr–Ar bonds, at $p \geq 20\%$, when practically each impurity atom has identical impurity atoms among its nearest neighbors, some quasi-continuous distribution of the weak bonds occurs in the lattice. In this case each region having the characteristic size $l \geq \lambda$ (sound wavelength) can be characterized by its own set of elastic constants, its own longitudinal and transverse sound velocities, which acquire a meaning of randomly distributed parameters.

No quasi-local low-frequency oscillations can occur in such systems. The low-frequency regions of the density of states of the $Kr_{1-p}Ar_p$ systems are shown in Fig. 4, the Ar concentrations being the same as in Fig. 1 (the curves are numbered as in Fig. 1; the dashed curve shows the density of states of ideal Kr from Ref. 13). In the frequency interval $\omega \leq \omega^*$ (the frequency of the first van Hove singularity) none of the curves has any sign of the characteristic quasi-local maximum. The curves have typical “quasi-Debye” shapes. In other words, the oscillations at these frequencies, which are responsible for the behavior of the heat capacity in the temperature interval 1–20 K, are completely delocalized.

At the same time, such systems with randomly distributed force and elastic parameters are noted for more inten-

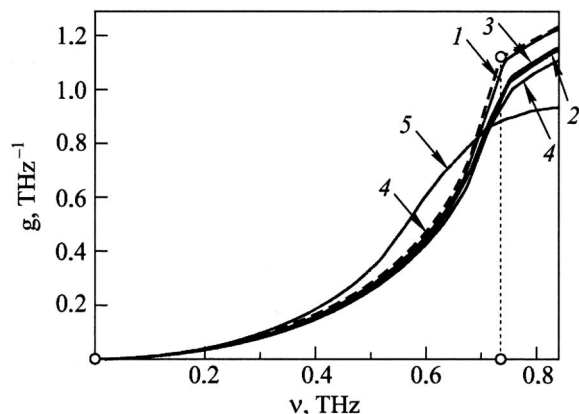


FIG. 4. Evolution of low-frequency regions (until the first van Hove singularity appears—the thin dashed vertical line) of the phonon densities of the $Kr_{1-p}Ar_p$ solution at a growing Ar concentration p . Heavy dashed curve—phonon density of pure Kr. The curves are numbered as in Fig. 1.

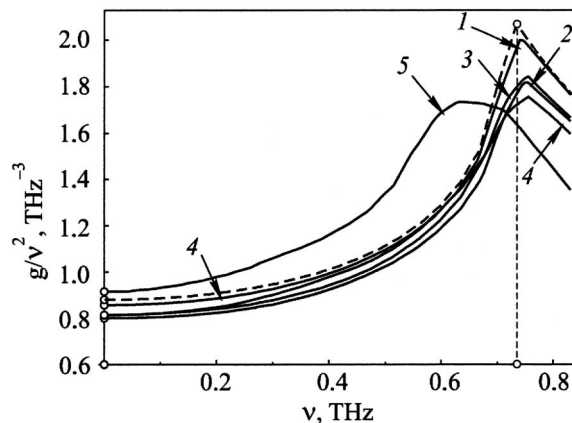


FIG. 5. Evolution of low-frequency $g(\nu)/\nu^2$ regions at a growing Ar concentration p in the $Kr_{1-p}Ar_p$ solid solution (the notation is the same as in Fig. 4).

sive sound wave dispersion. As a result, the curve $\nu(\omega)$ starts to deviate from the quadratic (Debye) behavior at lower temperatures. For this reason the ratio $\nu(\omega)/\omega^2$ reaches a maximum in glasses and some other disordered systems (e.g., the system in Ref. 27). This is the so-called “boson maximum” (or “boson peak”).^{6–11,27–32} Note that in these studies this peak was investigated mainly for the phonons with frequencies at which the sound velocity becomes dependent on the wave vector (from “propagons” to “diffusons” in the terminology of Ref. 33). The absence of a distinct boundary between the propagons and diffusons is usually identified with the Ioffe-Regel effect (see, e.g., Refs. 32 and 33).

However, even higher-frequency acoustic phonons whose dispersion ceases being linear (the so-called “diffusons”) can form a similar maximum if its frequency is not higher than ω^* .

Figure 5 illustrates the ratios $\nu(\omega)/\omega^2$ for $Kr_{1-p}Ar_p$. There is a maximum only at $p=50\%$. At other concentrations there is not enough time to form the maximum of the frequency of the first van Hove singularity—opening of isofrequency surfaces of transverse acoustic oscillations. However, as the propagation of the sound wave slows down, the number of low-frequency phonons (especially those with $k \rightarrow 0$) increases, and so does the low-temperature heat capacity. On the other hand, the number of low-frequency phonons decreases because of the small mass of the impurity atoms. It is natural that the two mechanisms—the increase and the decrease in the number of phonons—compete in Ar–Kr solutions. Note that at $p=24.4\%$ the maximum of the relative change in the heat capacity (Figs. 1 and 2) is negative, and it becomes positive only at higher Ar concentrations (e.g., see Fig. 1, curve 5).

Thus the analysis performed shows that at rather high Ar concentrations, the nonmonotonic temperature dependence of the relative change in the heat capacity of $Kr_{1-p}Ar_p$ solid solutions is determined by excitation of delocalized high-dispersion low-frequency phonons. In turn, the high-dispersion low-frequency phonons are due to the random distribution of weak bonds in the lattice, which are typical for the Ar–Ar interaction in this solution. Note that the distributed weak bonds cause a severe local anisotropy of the oscillations of both the Ar and Kr atoms. The local anisotropy

leads to some pushing of the phonons towards the ends of the band of the quasi-continuous spectrum, which increases the number of low-frequency phonons.

^{a)}E-mail: feodosiev@ilt.kharkov.ua

¹⁾The contributions from impurity clusters such as equilateral triangles and tetrahedrons, are qualitatively similar to the contributions made by impurity pairs; besides, the concentration of such *localized* defects is extremely low.

¹A. F. Prikhot'ko, V. G. Manzhelii, I. Ya. Fugol', Yu. B. Gaididei, I. N. Krupskii, V. M. Loktev, E. V. Savchenko, V. A. Slyusarev, M. A. Strzheimchny, Yu. Freiman, and I. I. Shansky, *Cryocrystals* [in Russian], Naukova Dumka, Kiev (1983).

²V. I. Peresada and E. S. Syrkin, *Fiz. Tverd. Tela (Leningrad)* **18**, 336 (1976) [*Sov. Phys. Solid State* **18**, 197 (1976)].

³E. T. Bruk-Levinson, I. A. Gospodarev, A. I. Zakharov, and E. S. Syrkin, *Izv. AN Bel. SSR* **3**, 78 (1988).

⁴S. B. Feodosyev, I. A. Gospodarev, V. I. Grishaev, A. M. Kosevich, O. V. Kotlyar, and E. S. Syrkin, *J. Low Temp. Phys.* **139**, 665 (2005).

⁵O. V. Kotlyar and S. B. Feodosyev, *Fiz. Nizk. Temp.* **32**, 343 (2006) [*Low Temp. Phys.* **32**, 256 (2006)].

⁶W. A. Phillips (ed.), *Amorphous Solids Low Temperature Properties*, Springer-Verlag, Berlin (1981).

⁷A. P. Sokolov, A. Kisliuk, D. Quitmann, and E. Duval, *Phys. Rev. B* **48**, 7692 (1998).

⁸A. P. Sokolov, L. Rossler, A. Kisliuk, and D. Quitmann, *Phys. Rev. Lett.* **71**, 2062 (1993).

⁹V. K. Malinovsky, V. N. Novikov, P. P. Parshin, A. P. Sokolov, and M. G. Zemlyanov, *Europhys. Lett.* **11**, 43 (1990).

¹⁰C. C. Yu and J. J. Freeman, *Phys. Rev. B* **36**, 7620 (1987).

¹¹W. Schrimacher, *Europhys. Lett.* **73**, 892 (2006).

¹²V. G. Manzhelii, A. I. Prokhvatilov, I. Ya. Minchina, and L. D. Yantsevich, *Handbook of Binary Solutions of Cryocrystals*, Begel House, New York, Wallingford (UK) (1996).

¹³S. B. Feodosyev, I. A. Gospodarev, V. O. Kruglov, and E. V. Manzhelii, *J. Low Temp. Phys.* **139**, 651 (2005).

¹⁴V. I. Peresada, in *Condensed Matter Physics* [in Russian], Vol. 2, FTINT AN Ukr. SSR, Kharkov (1968), p. 172.

¹⁵V. I. Peresada, V. N. Afanas'ev, and V. S. Borovikov, *Low Temp. Phys.* **1**, 227 (1975).

¹⁶R. Haydock, *Solid State Phys.* (H. Ehrenreich, F. Seitz, and D. Turnbull, eds., Academic Press, New York) **35**, 129 (1980).

¹⁷I. M. Lifshitz, S. A. Gredeskul, and L. A. Pastur, *Introduction to the Theory of Disordered Systems*, Wiley-Interscience, New York (1988).

¹⁸I. M. Lifshitz, *JETP* **44**, 1723 (1963).

¹⁹I. M. Lifshitz, *Usp. Fiz. Nauk* **83**, 617 (1964) [*Sov. Phys. Usp.* **7**, 549 (1965)].

²⁰I. M. Lifshitz, S. A. Gredeskul, and L. A. Pastur, *J. Stat. Phys.* **38**, 37 (1985).

²¹P. Lécuyer, "Efficient and portable combined random number generators," *Commun. ACM* **31**, 6 (1988).

²²A. Maradudin, *Solid State Phys.* **18**, 273 (1966); **19**, 1 (1966).

²³I. M. Lifshitz, *Dokl. Akad. Nauk SSSR* **48**, 83 (1945).

²⁴I. M. Lifshitz, *Zh. Éksp. Teor. Fiz.* **17**, 1076 (1948).

²⁵V. I. Peresada and V. P. Tolstoluzhskii, *Sov. J. Low Temp. Phys.* **3**, 383 (1977).

²⁶M. I. Bagatskii, E. S. Syrkin, and S. B. Feodosyev, *Sov. J. Low Temp. Phys.* **18**, 629 (1992).

²⁷V. Gurarrie and A. Atland, *Phys. Rev. Lett.* **94**, 245502 (2005).

²⁸D. A. Parshin, *Phys. Solid State* **36**, 991 (1994).

²⁹W. Schrimacher, G. Diezeman, and C. Ganter, *Phys. Rev. Lett.* **81**, 136 (1998).

³⁰V. L. Gurevich, D. A. Parshin, and H. R. Schroder, *Phys. Rev. B* **67**, 094203 (2003).

³¹A. I. Chumakov, I. Sergeev, U. van Burck, W. Schrimacher, T. Asthalter, R. Ruffer, O. Leupold, and W. Petry, *Phys. Rev. Lett.* **92**, 245508 (2004).

³²M. I. Klinger and A. M. Kosevich, *Phys. Lett. A* **295**, 31 (2002).

³³P. B. Allen, J. I. Feldman, J. Fabian, and F. Wooten, *Philos. Mag. B* **72**, 1715 (1999).

This article was published in English in the original Russian journal. Reproduced here with stylistic changes by AIP.